Dynamic Unified RANS-LES Simulations of Periodic Hill flow at High Reynolds Number

Reza Mokhtarpoor

Department of Mathematics
University of Wyoming
1000 E. Univ. Ave., Laramie WY 82071, USA
rmokhtar@uwyo.edu

Stefan Heinz

Department of Mathematics
University of Wyoming
1000 E. Univ. Ave., Laramie WY 82071, USA
heinz@uwyo.edu

Michael Stoellinger

Department of Mechanical Engineering
University of Wyoming
1000 E. Univ. Ave., Laramie WY 82071, USA
mstoell@uwyo.edu

ABSTRACT

In this paper we present a new, theoretically well based, dynamic hybrid RANS-LES method, referred to as dynamic linear unified model (DLUM). It is applied to a high Reynolds number flow involving both attached and separated flow regimes: a periodic hill flow is simulated at a Reynolds number of 37,000. Its performance is compared to pure LES, pure RANS, other hybrid RANS-LES, and experimental observations. It is shown that the use of this computational method offers huge cost reductions of very high Reynolds number flow simulations compared to LES, it is much more accurate than RANS, and more accurate than LES, which is not fully resolved. We identified the reason for the superior performance of our new dynamic hybrid RANS-LES method compared to LES: it is the model's ability to respond to a changing resolution with adequate turbulent viscosity changes by ensuring simultaneously a physically correct turbulence length scale specification under the presence of interacting RANS and LES modes.

INTRODUCTION

One of the biggest challenges of computational fluid dynamics is the accurate and feasible simulation of very high Reynolds number flows involving flow separation. Such simulations are needed, for example, to improve the optimization of aircraft flight and wind turbine performance. The application of direct numerical simulation (DNS) for such flow computations is infeasible for the foreseeable future, and large-eddy simulation (LES) also is computationally too expensive with respect to the majority of such applications (Spalart *et al.*, 1997). The alternative use of Reynolds-averaged Navier-Stokes (RANS) equations suffers from major shortcomings if such equations are applied to separated flows because of the inability of RANS equations to simulate coherent instantaneous turbulent motions (recirculation regions and vortex shedding), a typical feature of separated turbulent flows.

The most natural approach to overcome these problems is the combination of RANS and LES methods to take advantage of both the computational efficiency of RANS equations and the ability of LES to resolve large scale flow structures and to simulate coherent instantaneous structures. There is a huge variety of suggestions of how hybrid RANS-LES methods should be designed, see, for example (Spalart *et al.*, 1997; Travin *et al.*, 2000; Hedges *et al.*, 2002; Shur *et al.*, 2008; Spalart, 2009; Hamba, 2009; Tucker & Davidson, 2004; Schiestel & Dejoan, 2005; Menter & Egorov, 2010; De Langhe *et al.*, 2008; Breuer *et al.*, 2008; Fröhlich & Terzi, 2008; Fasel *et al.*, 2006; Rajamani & Kim, 2010; Fadai-Ghotbi *et al.*, 2010; Girimaji, 2006). The main problem of this research area is the understanding of basic mechanisms of a computational method that is neither RANS nor LES: the interplay of RANS and LES modes in hybrid RANS-LES methods. The latter interaction is often considered to be the reason for a suboptimal performance of hybrid RANS-LES methods, which may suffer, for example, from a lack of fluctuations at the inlet of LES regions, or a significant amount of fluctuations that disturb RANS solutions in RANS regions.

The purpose of this paper is to further explore the benefits of hybrid RANS-LES methods based on stochastic analysis (Heinz, 2003*a*,*b*, 2007, 2008; Heinz & Gopalan, 2012; Gopalan *et al.*, 2013; Heinz *et al.*, 2015; Kazemi & Heinz, 2016). Conceptually, this approach has several advantages. First, such equations are based on a stochastic turbulence model that honors the realizability constraint (Lumley, 1978; Schumann, 1977; Vachat, 1977), this means the constraint that an acceptable turbulence closure model be based on the statistics of a velocity field that is physically achievable or realizable. The realizability principle is proven to significantly contribute to the development of accurate turbulence models (Fureby & Tabor, 1997; Ghosal, 1999; Vreman *et al.*, 1994; Durbin & Speziale, 1994; Girimaji, 2004; Pope, 1985, 1994; Speziale *et al.*, 1993; Wouters *et al.*, 1996). Second, the underlying stochastic turbulence model implies a hierarchy of simpler models, which can be systematically derived. Third, with respect to hybrid RANS-LES methods, this modeling approach focuses the hybridization problem to the problem of how scale information is provided to the model, whereas the velocity field is described by the same equations applied in RANS and LES. Fourth, with respect to dynamic LES, this modeling approach enables a formulation of the dynamic coefficient calculation that is consistent with the derivation of LES equations.

So far, the approach described in the preceding paragraph was used separately for performing non-dynamic hybrid RANS-LES simulations of turbulent channel flows (Gopalan *et al.*, 2013) and swirling turbulent jet flows (Heinz *et al.*, 2015), and nonhybrid dynamic LES of turbulent channel flows (Heinz & Gopalan, 2012) and the turbulent Ekman layer (Kazemi & Heinz, 2016). The purpose of this paper is to present a new computational method: a hybrid RANS-LES model that involves LES dynamically. This computational method will be applied to high Reynolds number separated flows which were already used for several studies of the perfor-

mance of computational methods with respect to separated flow simulations. The following specific questions will be considered:

1. With respect to grids that enable resolving simulations, what is performance-wise the difference between the new hybrid RANS-LES model considered and dynamic LES?
2. With respect to much coarser grids, what is performance-wise the difference between the new hybrid RANS-LES model considered and dynamic LES?
3. What is the reason for different performances of dynamic LES and the new hybrid RANS-LES model?
4. With respect to both the new hybrid RANS-LES model considered and dynamic LES, how do the computational cost of these methods scale with the Reynolds number?

The paper is organized in the following way. First, the equations of the dynamic unified RANS-LES model are introduced. Then the flows considered are described. The performance of LES and DLUM model versions, will be presented. Finally, the conclusions are summarized.

GOVERNING EQUATIONS

The unified RANS-LES model is based on a realizable stochastic model for turbulent velocities (Heinz, 2003*a*,*b*, 2007, 2008; Gopalan *et al.*, 2013). The model implies the exact but unclosed filtered Navier-Stokes equations. This means, the conservation of mass and momentum equations implied by the stochastic velocity model. Governing equations for the unified RANS-LES model used in here in all details can be find in recently published paper (Mokhtarpoor *et al.*, 2016). The final version of conservation of mass and momentum equations reads

$$\frac{\partial \bar{U}_i}{\partial x_i} = 0, \tag{1}$$

$$\frac{\bar{D}U_i}{\bar{D}t} = -\frac{1}{\rho}\frac{\partial P}{\partial x_i} + 2\frac{\partial(\nu+\nu_t)\bar{S}_{ij}}{\partial x_j}. \tag{2}$$

Here, the overbar refers to ensemble-averaged (RANS) or space-averaged (LES) variables. $\bar{D}/\bar{D}t$ denotes the filtered Lagrangian time derivative, U_i denotes components of the velocity vector, $P = (\bar{p}/\rho + 2k/3)$ is the modified pressure, ρ is the constant fluid density, ν is the constant kinematic viscosity, and S_{ij} is the rate-of-strain tensor. For obtaining of Eq. (2), a linear SGS stress model τ_{ij} (Heinz, 2007) which implies an expression for the SGS stress $\tau_{ij} = 2/3k\delta_{ij} - 2\nu_t\widetilde{S}_{ij}$ where the turbulent viscosity is given by $\nu_t = 2(1-c_0)k\tau/3$. τ is the dissipation time scale of turbulence, and c_0 is a model constant that is specified below. The transport equation for turbulent kinetic energy k is derived as (Heinz, 2003*b*)

$$\frac{\bar{D}k}{\bar{D}t} = \frac{\partial}{\partial x_j}\left[(\nu+\nu_t)\frac{\partial k}{\partial x_j}\right] + \nu_t|\widetilde{S}|^2 - \frac{k}{\tau}, \tag{3}$$

where $|\widetilde{S}| = (2\widetilde{S}_{ij}\widetilde{S}_{ji})^{1/2}$ refers to the magnitude of the rate-of-strain tensor.

Coupling of RANS and LES model

Equations (2) and (3) are unclosed as long as the time scale τ is not defined. Usually applied RANS and LES equations can be recovered by using $\tau = \tau^{RANS}$ with $\tau^{RANS} = 1/\omega$ for the RANS case, and $\tau = \tau^{LES}$ with $\tau^{LES} = \Delta k^{-1/2}$ for the LES case, respectively. Here, Δ refers to the filter width, which is defined to be the large side filter, $\Delta = \Delta_{max} = \max(\Delta_x, \Delta_y, \Delta_z)$, and ω is the characteristic turbulence frequency. To provide ω we solve transport equation for the turbulent frequency (Bredberg *et al.*, 2002).

The unification of RANS and LES models is accomplished by introducing the unified time scale by the relation $\tau = min(\tau^{RANS}, \tau^{LES})$.

The dynamic linear unified model (DLUM)

The closure of Eqs. (2), (3) and turbulent frequency transport equation combined with the incompressibility constraint still requires the definition of $2(1-c_0)/3$ in the SGS viscosity. To clearly distinguish between parameter settings in RANS and LES regimes we introduce new parameters for $2(1-c_0)/3$ in RANS and LES modes,

$$\nu_t = \begin{cases} C_\mu k\tau^{RANS} & \text{RANS region} \\ C_d k\tau^{LES} & \text{LES region} \end{cases} \tag{4}$$

We can compute C_d dynamically if the equations are in LES mode. There is a variety of dynamic LES methods. The advantage of the approach used here is that the dynamic LES method can be designed fully consistent with the LES model applied (Heinz, 2008; Heinz & Gopalan, 2012). The stochastic model considered to derive the LES model is upscaled such that this upscaled stochastic model implies test-filtered LES equations. The upscaled stochastic model determines an algebraic model for the deviatoric Leonard stress, which enables the dynamic coefficient calculation based on minimizing the least-squares error. This implies for C_d the relation

$$C_d = -\frac{L^d_{ij}M_{ji}}{M_{kl}M_{lk}}. \tag{5}$$

Here, L^d_{ij} refers to the deviatoric component of the Leonard stress $L_{ij} = \widehat{\bar{U}_i\bar{U}_j} - \hat{\bar{u}}_i\hat{\bar{u}}_j$ (the hat refers to the test filtering), and M_{ij} is given by $M_{ij} = 2\Delta^T\sqrt{k^T}\hat{\bar{S}}_{ij}$, which involves the test-filter turbulent kinetic energy $k^T = L_{nn}/2$ and filter width on the test-filter level $\Delta^T = 2\Delta$.

In RANS mode, the use of a constant value for C_μ does not account for the damping effect of walls. We have used a new C_μ blending method for treating wall effects (Mokhtarpoor *et al.*, 2016).

PERIODIC HILL FLOW

We have considered the separated flow over a periodic hill flow which its geometry follows Mellen *et al.* (2000). Experimental studies of this flow at Reynolds number of $Re = 37{,}000$ has been carried out by Rapp & Manhart (2011). A water channel of eleven meters in length has been used in the Hydromechanik Laboratorium of the Technische Universität München. Hills having a height of $3.035h$ were installed in the rectangular channel (dimensions are given in terms of the hill height $h = 50mm$). The width of channel was chosen to be $18h$ to achieve homogeneity in spanwise direction. Ten hills with an inter-hill distance of $9h$ were installed inside the channel. Two-dimensional particle image velocimetry (PIV) and laser-Doppler anemometry (LDA) were used as measurement techniques.

Numerical simulations of this flow at $Re = 37{,}000$ have been performed by Chaouat & Schiestel (2013). They applied their PITM hybrid model (Chaouat & Schiestel, 2005) on grids ranging from 240×10^3 to 960×10^6 points. PITM simulation results were compared with RANS Reynolds stress model (RSM) results. The authors observed that in contrast to the PITM simulations, the RSM computations showed important weaknesses regarding the prediction of this flow caused by the lack of large unsteady eddies.

Figure 1 shows the computational domain applied in our simulations. The size of the computational domain is $L_x = 9h$, $L_y = 3.035h$, and $L_z = 4.5h$ in the streamwise, wall normal, and spanwise directions, respectively, where h is the height of the hill. The

Reynold number of the flow is 37,000 based on hill height and bulk velocity above the hill crest. At the bottom and top, the channel is constrained by solid walls. No-slip and impermeability boundary conditions are used at these walls. Periodic boundary conditions are employed in the streamwise and spanwise directions.

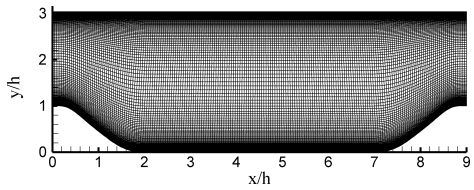

Figure 1: Computational domain of two-dimensional hill flow simulations: A sample curvilinear grid is shown.

RESULTS

In this section performance of DLUM model is presented in two parts. First, by comparing with LES model in different grids and second, by comparing with other DLUM versions that uses slightly different near wall treatment in RANS layer. Then the gray area problem is investigated for DLUM model.

DLUM vs. LES

We present a comparison of the performance DLUM vs LES models (LES on 20M, 5M, 500K grids, DLUM simulations on the 500K grid). First, we consider main flow charactristics by comparing streamlines and reattachment and separation points.

Table 1 summarizes the separation, reattachment points and percentage ε_{reatt} of discrepancy with the experimental data for LES and DLUM simulations. The comparison between DLUM and 20M LES results shows that the difference of reattachment and separation points is approximately the same. The difference is that the reattachment point provided by the DLUM is closer to the experimental result (Rapp & Manhart, 2011) than the 20M LES reattachment point. There is a difference between fine and coarser LES results regarding the reattachment and separation points: the coarser LES provide this distance 6.4% shorter than the fine grid LES. This indicates shortcomings of coarser LES to accurately simulate the recirculating bubble. Overall, we conclude that the DLUM performance is better than the performance of the fine grid LES considered.

The mean streamwise velocity $\langle U\rangle/U_b$ obtained by the DLUM simulation are compared with available experimental data and the three LES simulations considered (see Fig. 2). It is found that the DLUM shows an impressive ability to reflect the most important flow feature, the mean streamwise velocity. The comparisons with experimental data reveal an almost perfect performance of the DLUM

It is found that the DLUM shows an impressive ability to reflect the most important flow feature, the mean streamwise velocity. The comparisons with experimental data reveal an almost perfect performance of the DLUM in comparison with fine LES model.

DLUM vs. DLUM versions

In this section compare the three DLUM versions (DLUM, DLUM-NW, DLUM-FW), which do only differ by their conditioning on the ratio k_{mod}/k_{tot} of modeled to total kinetic energy in the near wall region where C_μ damping is applied (**?**). In particular, we consider their ability to respond to variations of k_{mod}/k_{tot} with turbulent viscosity changes. It helped us to find a best wall treatment for RANS layer.

Table 1: Location of separation and reattachment points obtained by DLUM and LES simulations on different grids.

Simulation	N_{cell}	x/h_{sep}	x/h_{reatt}	ε_{reatt}
LES 20M grid	20 M	0.23	3.65	3%
LES 5M grid	5 M	0.24	3.5	7%
LES 500K grid	500 K	0.3	3.5	7%
DLUM 500K grid	500 K	0.35	3.8	1%

The differences of DLUM versions is addressed in Fig. 3, which shows contour plots of the turbulent viscosity ratio $\langle \nu_t/\nu\rangle$ and k_{mod}/k_{tot}. Due to the fact that k_{mod}/k_{tot} variations take place in thin layers close to the wall, we do not find extended k_{mod}/k_{tot} variations over all the flow field as given with respect to viscosities. As expected, the largest variations of k_{mod}/k_{tot} take place immediately after separation at about $x/h = 0.5$.

Let us compare first the DLUM-NW and DLUM features. The DLUM implies at about $x/h = 0.5$ a more extended area of relatively low resolution (high k_{mod}/k_{tot}) compared to the DLUM-NW. It is very interesting to see that the DLUM treats the down-hill near wall region as a less resolved area. The differences of k_{mod}/k_{tot} variations given by the DLUM-NW and DLUM, which may appear to be relatively small, have a clear effect on the turbulent viscosity distributions. In contrast to the DLUM-NW, the DLUM treats the down-hill near wall region in a much more balanced way as an area of relatively low resolution and corresponding high turbulent viscosity. Otherwise, it is relevant to note that the overall viscosity distribution is not affected and basically equal for the DLUM-NW and DLUM. Compared to the DLUM, the DLUM-FW further extends the areas of relatively low resolution, in particular in the down-hill near wall region. As can be expected, this leads to a further increase of viscosity in the down-hill near wall region. However, the much more dominant effect is a significant change of the overall viscosity distribution. The increased viscosity accumulation near the wall implies a viscosity reduction in most of the other flow: we see larger (blue) areas of relatively small viscosities and smaller (green and red) areas of relatively high viscosities. Compared to the DLUM, neither the imbalanced treatment of the down-hill near wall region implied by the DMUL-NW nor the more imbalanced overall viscosity distribution implied by the DLUM-FW can be expected to contribute to better flow predictions. It turns out that the differences of DLUM versions discussed in the preceding paragraph imply a different performance in simulations. This is demonstrated in terms of Fig. 4, which shows mean velocities and stresses of DLUM versions in comparison to corresponding pure RANS and LES results on the same grid. First, compared to the DLUM it is surprising to see that the DLUM-NW and DLMU-FW have a relatively limited effect on the stresses. However, there are clear deficiencies of DLUM-NW and DLMU-FW mean velocities. In particular, we see that the DLUM-NW and DLUM-FW produce velocities that are relatively similar to the velocities of pure LES and RANS, respectively. This can be explained by the relatively small and relatively high turbulent viscosities of the DLUM-NW and DLUM-FW, respectively. What causes such LUM-NW and DLMU-FW deficiencies? The significant difference between the DLUM and DLUM-NW and DLMU-FW is that the DLUM ensures a physically correct length scale specification, in particular, under the presence of interacting RANS and LES modes (which poses a nontrivial problem, see the discussion in Sect. 5.1). In combination with the ability

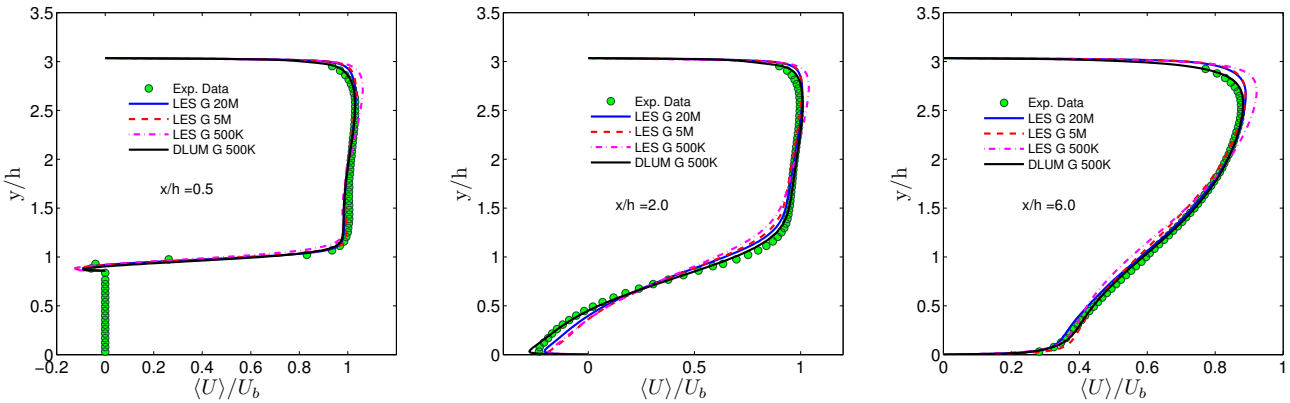

Figure 2: DLUM versus dynamic LES on different grids and experimental results: profiles of the streamwise velocity $\langle U \rangle / U_b$ are shown at different axial positions.

to respond with turbulent viscosity variations to resolution changes, the latter requirement appears to be the essential condition to ensure an optimal performance of a hybrid RANS-LES model.

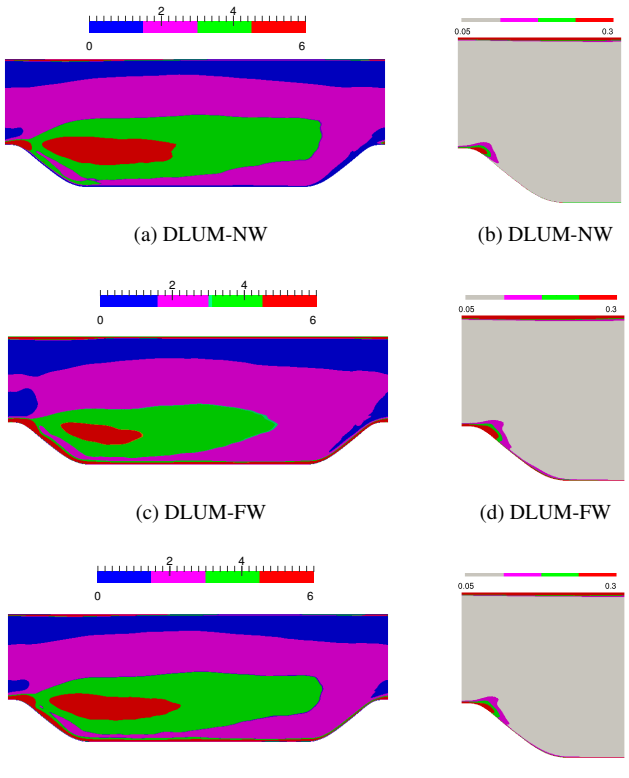

(a) DLUM-NW (b) DLUM-NW

(c) DLUM-FW (d) DLUM-FW

(e) DLUM (f) DLUM

Figure 3: Comparison of DLUM versions: contour plots of the turbulent viscosity ratio $\langle \nu_t / \nu \rangle$ (left) and the ratio k_{mod}/k_{tot} of modeled to total turbulent kinetic energy (right) obtained by the three DLUM versions.

Gray area problem

We finish this discussion with a general remark on the difference between the DLUM and other hybrid RANS-LES methods. The gray area problem is often seen to be the most challenging problem of developing hybrid RANS-LES methods. The gray area refers to the transition zone of regions that are treated as RANS and LES, this means the zone where we have difficulties to explain which type of simulation is actually applied. The term gray area problem refers to problems arising from the treatment of this transition zone. In particular, we may see a lack of fluctuations in the entrance region of LES-dominated regions, leading to a decreased ability of LES to resolve motions. Or, we may see an excess of fluctuations in RANS-dominated regions, leading to performance shortcomings because RANS equations are not designed to deal with a significant amount of fluctuations. The DLUM results reported here do not give any indication of a gray area problem related to the DLUM. The same applies if this problem is considered from a theoretical view point. The DLUM can be seen as dynamic LES where RANS is used to dynamically adjust the turbulent viscosity to a changing flow resolution. In this way, LES and RANS are not used as independent computational methods that need to be merged. Therefore, there is no reason to expect a gray zone problem because a gray zone does not exist. The gray area problem is usually addressed by asking whether the hybrid RANS-LES model considered implies a log-law mismatch, this means significant deviations from the log-law mean velocity profile, see, e.g., Ref. Gopalan *et al.* (2013). To provide further evidence for the view presented in the preceding paragraph, we consider the mean velocity profile close to the wall. Due to the presence of the recirculation region, there is no log-law-like behavior of the mean velocity close to the lower wall. Characteristic mean velocity variations close to the upper wall are shown in wall-units at $x/h = (0.5, 6)$ in Fig. 5 by including the log-law indicator function $I = dU^+/dln(y^+)$. It may be seen that there are significant differences between the DLUM predictions and the corresponding behavior seen in channel flow without hills: the typical $U^+ = y^+$ variation in the viscous layer is missing, and U^+ is much higher than seen in regular channel flow. These differences can be attributed to the DLUM grid resolution and the hill-induced high velocity values in the upper half of channel flow here, see Fig. 2, respectively. In particular for $x/h = 6$, the log-law indicator function indicates a log-law-like mean velocity variation close to the wall. Unfortunately, experimental data are missing in this flow region. However, the most important observation is the following: a log-law mismatch produced by any hybrid RANS-LES model is always also seen by a significant velocity over-prediction in the defect layer, but in this flow region we see an excellent agreement between DLUM results and experimental data. Thus, this comparison does also support the view that the DLUM does not suffer from the gray area problem.

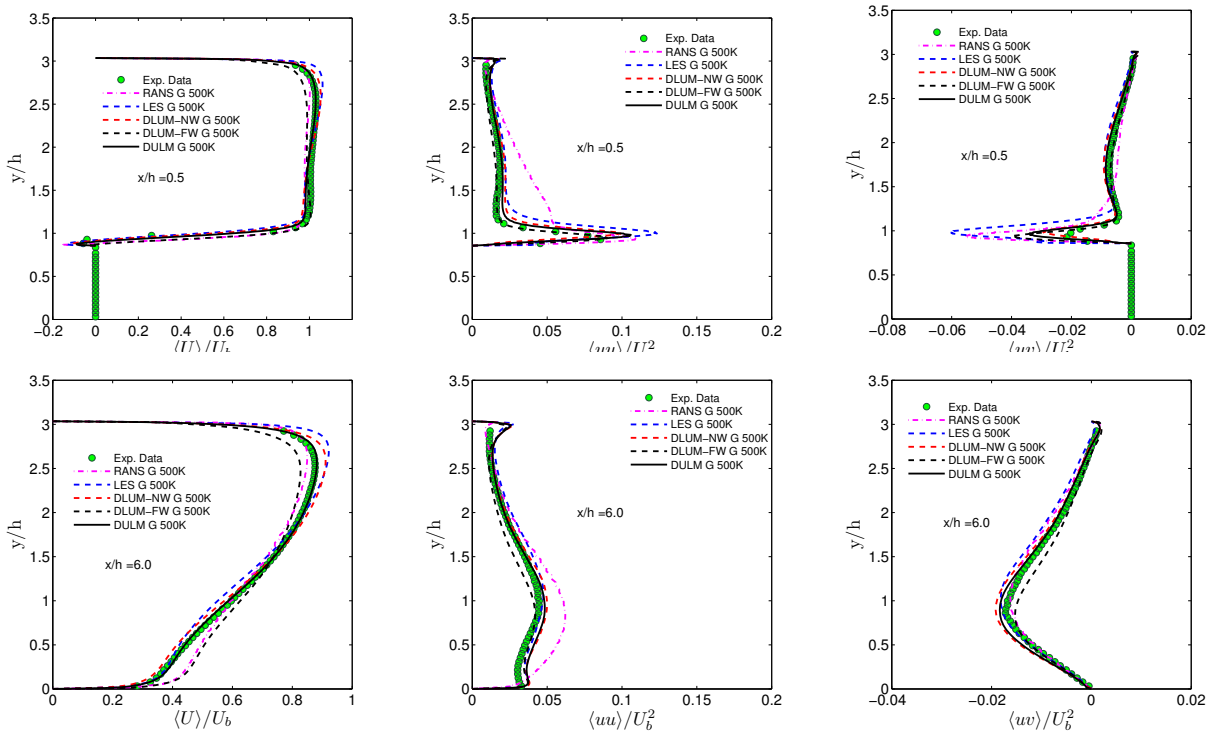

Figure 4: Comparison of the performance of the three DLUM versions versus RANS, dynamic LES, and experimental data: mean velocities and Reynolds stresses are shown at $x/h = (0.5, 6)$.

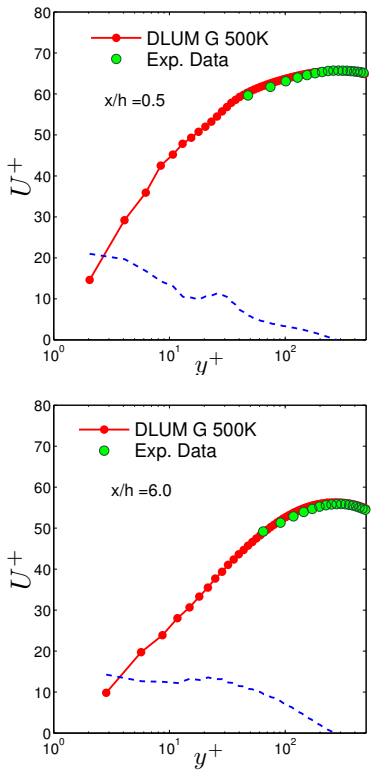

Figure 5: Mean velocity U^+ in wall-units versus $ln(y^+)$: Comparison of DLUM results and experimental data at x/h = (0.5, 6). Here, y^+ refers to the distance to the upper wall in wall-units. The blue line shows the log-law indicator function $I = dU^+/dln(y^+)$.

CONCLUSIONS

A new hybrid RANS-LES method is presented by combining of a hybrid RANS-LES method with dynamic LES. The hybrid RANS-LES model presented here is efficient for very high Reynolds number flow simulations compared to LES, it is much more accurate than RANS, and more accurate than under-resolved LES. From a more general view point, the DLUM is more reliable than LES for high Reynolds number flows, which often faces the nontrivial question (Davidson, 2009, 2010) of how well resolving the LES actually is. We identified the reason for the superior performance of the DLUM compared to LES: it is the DLUM ability to respond to a changing resolution with adequate turbulent viscosity changes by ensuring simultaneously a physically correct turbulence length scale specification under the presence of interacting RANS and LES modes. Based on conceptual arguments and our simulation results, we also concluded that our DLUM does not suffer from the gray area problem, which is usually considered to represent the biggest challenge of hybrid RANS-LES methods. Obviously, it would be highly beneficial to obtain more evidence for the advantages of the DLUM with respect to highly complex and very high Reynolds number flow simulations.

ACKNOWLEDGMENTS

The authors would like to acknowledge support through NASA's NRA research opportunities in aeronautics program (Grant No. NNX12AJ71A). We are very thankful for computational resources provided by the Advanced Research Computing Center and the Wyoming-NCAR Alliance at the University of Wyoming.

REFERENCES

Bredberg, J., Peng, S. H. & Davidson, L. 2002 An improved k-ω turbulence model applied to recirculating flows. *International Journal of Heat and Fluid Flow* **23** (6), 731–743.

Breuer, M., Jaffrézic, B. & Arora, K. 2008 Hybrid LES-RANS technique based on a one-equation near-wall model. *Theoretical and Computational Fluid Dynamics* **22** (3), 157–187.

Chaouat, B. & Schiestel, R. 2005 A new partially integrated transport model for subgrid-scale stresses and dissipation rate for turbulent developing flows. *Phys. Fluids* **17**, 1–19.

Chaouat, B. & Schiestel, R. 2013 Hybrid rans/les simulations of the turbulent flow over periodic hills at high reynolds number using the pitm method. *Computers and Fluids* **84**, 279–300.

Davidson, L. 2009 Large eddy simulations: how to evaluate resolution. *International Journal of Heat and Fluid Flow* **30** (5), 1016–1025.

Davidson, L. 2010 How to estimate the resolution of an LES of recirculating flow. *Quality and Reliability of Large-Eddy Simulations II* **16**, 269286.

De Langhe, C., Bigda, J., Lodefier, K. & Dick, E. 2008 One-equation rg hybrid rans/les computation of a turbulent impinging jet. *Journal of Turbulence* **9** (16), 1–19.

Durbin, P. A. & Speziale, C. G. 1994 Realizability of second-moment closure via stochastic analysis. *Journal of Fluid Mechanics* **280**, 395–407.

Fadai-Ghotbi, A., Friess, C., Manceau, R. & Borée, J. 2010 A seamless hybrid rans-les model based on transport equations for the subgrid stresses and elliptic blending. *Physics of Fluids* **22**, 055104.

Fasel, H. F., Terzi, D. A. Von & Sandberg, R. D. 2006 A methodology for simulating compressible turbulent flows. *Journal of Applied Mechanics* **73** (3), 405–412.

Fröhlich, J. & Terzi, D. V. 2008 Hybrid LES/RANS methods for the simulation of turbulent flows. *Progress in Aerospace Sciences* **44** (5), 349–377.

Fureby, C. & Tabor, G. 1997 Mathematical and physical constraints on large-eddy simulations. *Theoretical and Computational Fluid Dynamics* **9** (2), 85–102.

Ghosal, S. 1999 Mathematical and physical constraints on large-eddy simulation of turbulence. *AIAA Journal* **37** (4), 425–433.

Girimaji, S. S. 2004 A new perspective on realizability of turbulence models. *Journal of Fluid Mechanics* **512**, 191–210.

Girimaji, S. S. 2006 Partially-Averaged Navier-Stokes model for turbulence: a Reynolds-Averaged Navier-Stokes to Direct Numerical Simulation bridging method. *J. Appl. Mech.* **73**, 413–421.

Gopalan, H., Heinz, S. & Stöllinger, M. 2013 A unified RANS-LES model: Computational development, accuracy and cost. *Journal of Computational Physics* **249**, 249–274.

Hamba, F. 2009 Log-layer mismatch and commutation error in hybrid rans/les simulation of channel flow. *International Journal of Heat and Fluid Flow* **30** (1), 20–31.

Hedges, L. S., Travin, A. K. & Spalart, P. R. 2002 Detached-eddy simulations over a simplified landing gear. *Journal of Fluids Engineering* **124** (2), 413–423.

Heinz, S. 2003*a* On Fokker–Planck equations for turbulent reacting flows. Part 2. Filter density function for large eddy simulation. *Flow, Turbulence and Combustion* **70** (1), 153–181.

Heinz, S. 2003*b* *Statistical Mechanics of Turbulent Flows*, 1st edn. Springer-Verlag, Berlin, Heidelberg, New York, Tokyo.

Heinz, S. 2007 Unified turbulence models for LES and RANS, FDF and PDF simulations. *Theoretical and Computational Fluid Dynamics* **21** (2), 99–118.

Heinz, S. 2008 Realizability of dynamic subgrid-scale stress models via stochastic analysis. *Monte Carlo Methods and Applications* **14** (4), 311–329.

Heinz, S. & Gopalan, H. 2012 Realizable versus non-realizable dynamic subgrid-scale stress models. *Physics of Fluids* **24** (11), 115105/1–23.

Heinz, S., Stoellinger, M. & Gopalan, H. 2015 Unified RANS-LES Simulations of Turbulent Swirling Jets and Channel Flows. In *Progress in Hybrid RANS-LES Modelling (Notes on Numerical Fluid Mechanics and Multidisciplinary Design 130)*, pp. 265–275. Cham, Heidelberg, New York, Dordrecht, London: Springer.

Kazemi, E. & Heinz, S. 2016 Dynamic large eddy simulations of the ekman layer based on stochastic analysis. *Int. J. Nonlinear Sciences Numerical Simulation (in press)* .

Lumley, J. L. 1978 Computational modeling of turbulent flows. *Advances in Applied Mechanics* **18**, 123–175.

Mellen, C. P., Frohlich, J. & Rodi, W. 2000 Large-eddy simulation of the flow over periodic hills. In *Proceedings of 16th IMACS world congress*, pp. 1–6. Lausanne, Switzerland.

Menter, F. R. & Egorov, Y. 2010 The scale-adaptive simulation method for unsteady turbulent flow predictions. Part 1: theory and model description. *Flow Turbul. Combust.* **85**, 113–138.

Mokhtarpoor, R., Heinz, S. & Stoellinger, M. 2016 Dynamic unified rans-les simulations of high reynolds number separated flows. *Phys. Fluids* **28**, 095101.

Pope, S. B. 1985 PDF methods for turbulent reactive flows. *Progress in Energy and Combustion Science* **11** (2), 119–192.

Pope, S. B. 1994 On the relationship between stochastic lagrangian models of turbulence and second-moment closures. *Physics of Fluids* **6** (2), 973–985.

Rajamani, B. & Kim, J. 2010 A hybrid-filter approach to turbulence simulation. *Flow, Turbulence and Combustion* **85** (3-4), 1–21.

Rapp, C. & Manhart, M. 2011 Flow over periodic hills – an experimental study. *Exp. Fluids* **51**, 247–269.

Schiestel, R. & Dejoan, A. 2005 Towards a new partially integrated transport model for coarse grid and unsteady turbulent flow simulations. *Theoret. Comput. Fluid Dynamics* **18**, 443–468.

Schumann, U. 1977 Realizability of reynolds stress turbulence models. *Physics of Fluids* **20** (5), 721–725.

Shur, M.L., Spalart, P.R., Strelets, M. & Travin, A. 2008 A hybrid RANS-LES mmodel with delayed DES and wall-modeled LES capabilities. *Int. J. Heat Fluid Flow* **29**, 1638–1649.

Spalart, P.R. 2009 Detached-eddy simulation. *Annual Review of Fluid Mechanics* **41** (2), 181–202.

Spalart, P. R., Jou, W. H., Strelets, M. & Allmaras, S. R. 1997 Comments on the feasibility of LES for wings, and on a hybrid RANS/LES approach. In *1st AFOSR Intl. Conf. on DNS/LES*, pp. 4–8. Ruston, LA, USA: Columbus: Greyden Press.

Speziale, C. G., Abid, R. & Durbin, P. A. 1993 New results on the realizability of Reynolds stress turbulence closures. *ICASE Report* **93-76**, 1–47.

Travin, A., Shur, M., Strelets, M. & Spalart, P. 2000 Detached-eddy simulations past a circular cylinder. *Flow, Turbulence and Combustion* **63** (1), 293–313.

Tucker, P. G. & Davidson, L. 2004 Zonal k–l based large eddy simulations. *Computers and Fluids* **33** (2), 267–287.

Vachat, R. Du 1977 Realizability inequalities in turbulent flows. *Physics of Fluids* **20** (4), 551–556.

Vreman, B., Geurts, B. & Kuerten, H. 1994 Realizability conditions for the turbulent stress tensor in large-eddy simulation. *Journal of Fluid Mechanics* **278**, 351–362.

Wouters, H. A., Peeters, T. W. J. & Roekaerts, D. 1996 On the existence of a generalized Langevin model representation for second-moment closures. *Physics of Fluids* **8** (7), 1702–1704.